π-Conjugation and End Group Effects in Long Cumulenes: Raman Spectroscopy and DFT Calculations

Matteo Tommasini,*[,†] Alberto Milani,[†] Daniele Fazzi,[‡] Andrea Lucotti,[†] Chiara Castiglioni,[†] Johanna A. Januszewski,[§] Dominik Wendinger,[§] and Rik R. Tykwinski[§]

[†]Dipartimento di Chimica, Materiali e Ingegneria Chimica—Politecnico di Milano, Piazza Leonardo da Vinci 32, 20133 Milano, Italy

[‡]Max-Planck-Institut für Kohlenforschung, Kaiser-Wilhelm-Platz 1, 45470 Mülheim, Germany

[§]Department of Chemistry and Pharmacy & Interdisciplinary Center of Molecular Materials (ICMM), Friedrich-Alexander-Universität Erlangen-Nürnberg (FAU), Henkestrasse 42, 91054 Erlangen, Germany

INTRODUCTION

Carbon is a very versatile element, which shows different allotropic forms thanks to its possible hybridization states. sp-Hybridized carbon atoms can organize themselves in the form of one-dimensional atomic chains, which have been observed in a variety of environments, such as, for instance, in plants, in fungal and marine sources,[1−3] in meteorites,[4,5] in interstellar dust,[6] in mixed sp/sp^2 carbon nanostructures,[7−9] or inside carbon nanotubes[10,11] and between graphitic domains.[12] sp-Carbon chains with different terminations and chain lengths have been prepared by means of different chemical/physical techniques, namely solution-phase synthesis,[13−19] laser irradiation of graphite,[20] or gas-phase deposition methods.[7,8] The sp-carbon systems share some features with sp^2 π-conjugated systems (graphene, carbon nanotubes) and show tunable structure-, length-, and termination-dependent properties. Considering the ideal infinite chain (i.e., carbyne), two possible limiting structures can be defined, which possess an equalized geometry (all double bonds, i.e., polycumulene) or an alternated geometry (single/triple bonds, i.e., polyyne). The two structures display, respectively, a metallic or semiconducting character. Many efforts have been devoted to the synthesis of increasingly long sp-carbon chains, aiming at reaching, as closely as possible, the carbyne limit.[21−25] By adopting different end-capping groups, it has been possible to stabilize these intrinsically reactive systems. Furthermore, end groups proved to be able to affect the structure of the whole sp chain, tuning its conjugation properties.[26−28] However, the majority of the sp systems reported so far possess an alternated structure in the ground state (polyynic), even if cumulenic geometries have been induced by electronic excitation[29] or charge transfer processes.[28] This situation has recently changed since stable cumulenic chains with a maximum length of 10 carbon atoms have been synthesized, as model compounds for an alternative route toward carbyne.[24,25] The control of the molecular structure and the tuning of the cumulenic vs polyynic configuration are important not only from the point of view of the synthesis but also for the new perspectives that it may open for innovative applications. Promising properties have been reported on the basis of theoretical predictions of the conductance of cumulenes and polyynes[30,31] Several other potential applications have been proposed, as active materials in nanoelectronic or spintronic devices,[32] as nonlinear optical materials,[33−36] as molecular wires,[26,37−45] and even as the

Received: September 25, 2014
Revised: October 9, 2014
Published: October 10, 2014

stiffest known material.[32] Recent calculations have also revealed that in nanostructured hybrid sp/sp^2 systems interesting interactions between sp and sp^2 domains take place,[46] opening the way for the design of tailored systems for molecular electronics (for instance, the main result of our present work is consistent with this expected behavior). Within this context, the characterization of cumulenic sp-carbon chains is mandatory for the interpretation of their still unexplored features. As for other π-conjugated carbon systems, vibrational spectroscopy, and Raman scattering in particular, is a powerful technique for the basic investigation of the structural, vibrational, and electronic properties of sp-carbon chains[9,27−29,36,47−51] This work presents a comparative analysis of the infrared and Raman spectra of newly synthesized long cumulenes.[24,25] We aim at identifying specific spectral markers that could be taken as signatures of a structure characterized by a linear sequence of cumulated CC double bonds. The interpretation of experiments through DFT calculations reveals a particularly significant influence of the end groups on the molecular and electronic structure and on the spectroscopic response. These results provide valuable information for the characterization of nanostructured carbon systems containing sp carbon nanowires.

EXPERIMENTAL SECTION

The synthesis of the cumulenes under investigation, namely end-capped di(*tert*-butyl)phenyl [*n*]cumulenes, *n* = 3, 5, 7, 9 (hereafter referred to as [*n*]tBuPh, *n* being the number of cumulated double bonds in the linear chain) and end-capped mesityl or 2,4,6-trimethylphenyl[9]cumulene ([9]Mes), is reported in ref 24. In this work we also consider a series of symmetric polyynes, characterized by similar end groups, namely end-capped di(*tert*-butyl)phenyl polyynes, SP(*N*), *N* = 4−20 (*N* being the number of triple bonds in the polyyne chain), recently analyzed by vibrational spectroscopy[50] and synthesized as described in ref 17.

Vibrational spectra have been recorded with FT-IR and FT-Raman equipment (respectively, Nicolet NEXUS with micro-IR setup Thermo Nicolet Continuμm and MCT detector; Nicolet NXR9650, excitation at 1064 nm from Nd-YVO4 laser). For spectroscopy measurements, cumulene solutions in diethyl ether were obtained right after the last step of the chemical synthesis. This was carried out in the Politecnico di Milano spectroscopy laboratories by two of us (J.A.J. and D.W.), directly starting from stable cumulene precursors previously synthesized in the Erlangen laboratories. This experimental procedure minimizes the time delay between chemical synthesis and spectroscopy measurements, which typically occur within 5 min after synthesis. This approach grants fresh material for which degradation issues are negligible. In fact, the time evolution of all spectra was measured over a total period of about 30 min to 1 h, in order to assess the presence of any time-dependent spectral features, which could be assigned to degradation processes of the cumulene species. The spectra reported in this paper are those recorded at the earliest times for which no detectable signals associated with degradation products have been found, to the best of the authors' judgment. In order to avoid the presence of solvent bands in vibrational spectra, which requires a delicate treatment of the data aimed at compensating the solvent features, we have focused our analysis on the spectra recorded on fresh solid-state samples of the pure cumulenes. Solid deposits on substrates suitable for IR and Raman spectroscopy (diamond anvil cell and aluminum foil, respectively) have been directly obtained by solvent evaporation from small droplets of the cumulene solution immediately after the last step of the chemical synthesis. It is worth reporting that the vibrational spectra from solution and solid state are very similar in the CC stretching region associated with sp-chain signals (where the compensation of solvent peaks is most reliable). This is expected, since cumulene crystals are characterized by a low density, due to the presence of bulky end groups, which prevents a close packing of the carbon chains and minimizes interchain interactions.[24] For SP[*N*] polyynes FT-Raman measurements have been carried out on as-received solids from chemical synthesis; FT-IR measurements have been carried out on the same powders with diamond anvil cell and micro-IR setup.

Theoretical calculations have been carried out within Density Functional Theory (DFT) at the PBE0/6-311G** level. DFT has proved to be useful for investigating the structure and spectroscopic properties of sp-carbon chains.[27−29,50−53]

The Gaussian09 code[54] has been used to carry out all quantum chemical calculations here presented. A suite of in-house developed computer codes have been used to postprocess the numerical data contained in the Gaussian09 formatted checkpoint and output file (further details on the procedure and examples of application can be found in refs 55−57). In this way we obtain local Raman parameters, simulations of Raman spectra, and the graphical representations of the nuclear displacements of selected normal modes.

MOLECULAR STRUCTURES

Figure 1 reports the structure of the molecules investigated in this work. X-ray diffraction analysis carried out for the [*n*]tBuPh series and for [9]Mes[24] has revealed that, in solid state, these molecules, compared with polyynes, exhibit a fairly low Bond Length Alternation (BLA) along the carbon chain. The cumulene chains are also fairly linear (CCC angles rarely vary

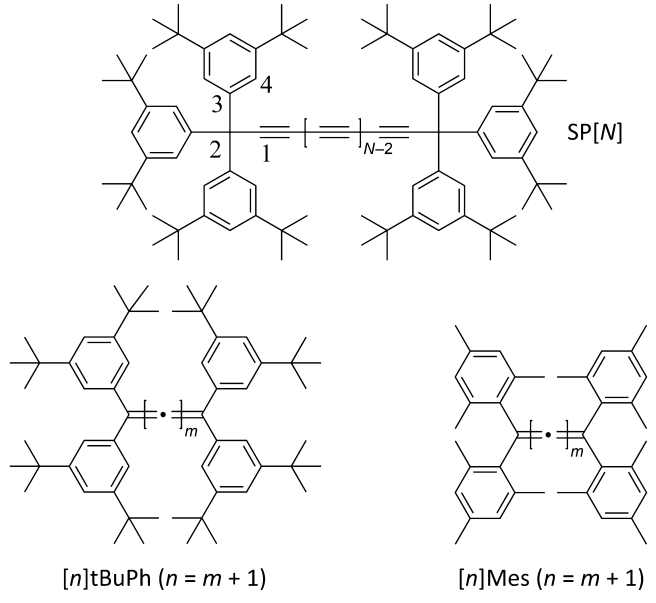

Figure 1. Structures of the molecules discussed in this paper. Polyynes: SP[*N*] (*N* = number of triple bonds); Cumulenes: [*n*]tBuPh (*n* = number of cumulated double bonds, *n* = *m* + 1) and [*n*]Mes. The sequence of atoms 1, 2, 3, 4 defines the aryl twist conformation for all the molecules considered (see text).

by more than a few degrees from the value of 180°, typical of ideal sp-hybrids). Optimized molecular structures have been determined by means of DFT calculations on isolated molecules. Figure 2 reports the comparison of the cumulene

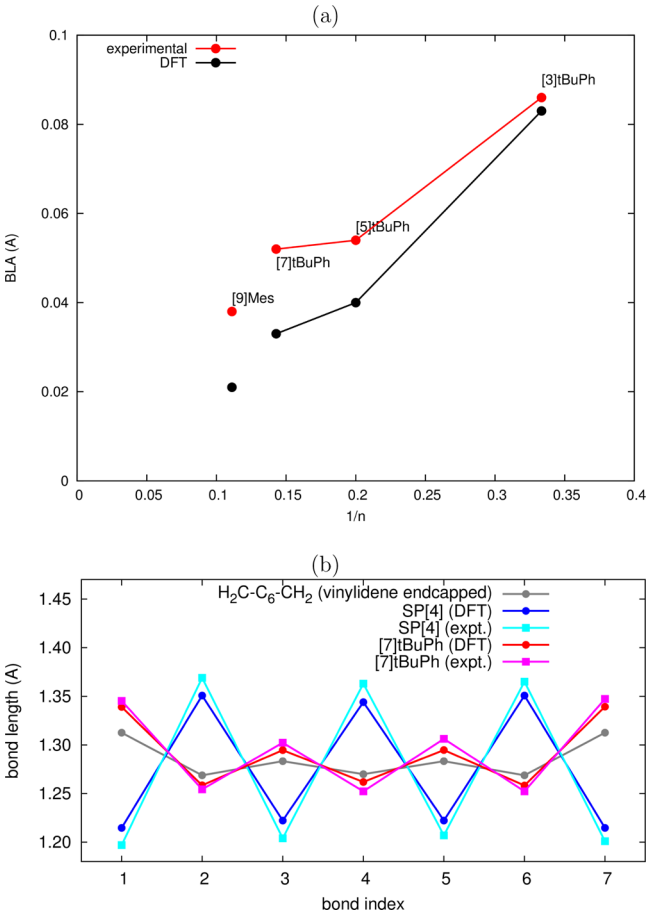

Figure 2. (a) Comparison between experimental[24] and DFT (PBE0/6-311G**) computed BLA of [*n*]tBuPh. The BLA values have been determined considering the difference of the equilibrium bond lengths of the central CC bonds and that of the adjacent bond. (b) CC bond lengths along different linear carbon chains made by seven conjugated CC bonds: [7]tBuPh (expt. and theo.), vinylidene end-capped cumulene $CH_2-C_6-CH_2$ (theo.), and SP[4] polyyne (expt.[58] & theo.).

CC bond length pattern predicted by DFT versus experimental observation (X-ray diffraction data are reported in ref 24). Overall there is fairly good agreement. Since DFT results are for isolated molecules, this fact indirectly confirms that the presence of bulky end groups prevents intermolecular interactions in the solid state that could affect the bond alternation pattern.

In Figure 2a we plot the values of the BLA parameter obtained considering the length difference between the central CC bond and the adjacent one, for all the cumulene molecules considered in this work (i.e., [*n*]tBuPh, with *n* = 3, 5, 7 and[9]Mes). Theoretical and experimental values are close and show a similar trend, demonstrating that, starting from five cumulated double bonds, BLA values become very small. It is interesting to notice that the BLA values of [9]Mes are shifted toward lower values with respect to the trend shown by the [*n*]tBuPh series. This indicates that end groups influence to some extent the structure of the carbon chain: mesityl groups induce a stronger equalization of the carbon chain, as already noticed in ref 24.

Figure 2b compares the pattern of CC bond lengths in three differently capped sp-carbon chains. The molecules have been selected on the basis of the number of conjugated CC bonds in the chain, which is defined by the sequence of carbon atoms carrying 2p electrons (i.e., C in sp or sp^2 hybridization in the case of the end carbons in cumulenes). Accordingly the number of conjugated CC bonds in SP[*N*] polyynes is $2N - 1$ while in [*n*]tBuPh it is equal to *n* (see Figure 1). The three molecules in Figure 2b consist of seven conjugated CC bonds. The two cumulenes ([7]tBuPh and vinylidene end-capped $CH_2-C_6-CH_2$) display rather close bond length values, characterized by a low degree of bond alternation. However, a small end-group dependence is revealed by the bond length patterns, which indicates that vinylidene groups induce more efficient bond equalization compared to tBuPh substituents. As expected for polyynes, such as SP[4], the CC bond length pattern is clearly different from that of the two cumulenes, and it can be described in terms of an ideal structure with alternated triple and single bonds.

EXPERIMENTAL VIBRATIONAL SPECTRA

In Figures 3 and 4, experimental IR and Raman spectra of [*n*]tBuPh (*n* = 3, 5, 7) and [9]Mes are reported in comparison with the analogous data for the polyyne series SP[*N*]. Figure 5 shows a direct comparison between the vibrational spectra of carbon chains featuring the same number of conjugated bonds, such as SP[4] and [7]tBuPh. This close-up representation is useful to discuss the remarkable spectroscopic differences between polyynic and cumulenic systems.

For both polyynes and cumulenes the IR spectra are dominated by the structured CH stretching band of *tert*-butyl groups (2800−3000 cm^{-1}), which is accompanied by weak features associated with aromatic CH stretchings (above 3000 cm^{-1}).[62] Stretching and bending modes mainly localized on tBuPh groups occur in the 1300−1650 cm^{-1} region, which shows a persistent spectral pattern for both the cumulene [*n*]tBuPh series and the polyyne SP[*N*] series. This is expected since similar end-capping groups characterize both series. However, non-negligible spectroscopic changes in this region can be observed for [9]Mes, due to the presence of methyl groups directly linked to the aromatic rings.

Infrared active CC stretching transitions assigned to the conjugated sp-carbon chains give rise to relatively weak features in the 2000 cm^{-1} region. Comparing SP[4] and [7]tBuPh, we observe a remarkable shift of the CC stretching band to lower cm^{-1}, from 2215 cm^{-1} (SP[4]) to 2055 cm^{-1} ([7]tBuPh), as expected in the presence of a more "metallic" structure for the cumulene chain.[53]

In Figure 3a one clearly observes that the number of IR bands assigned to the sp-carbon chain increases with increasing chain length. The appearance of this sequence of bands in the 2000−2500 cm^{-1} region has been interpreted in the frame of the classical "oligomer approach", which allows correlation of vibrational frequencies of oligomers (SP[*N*]) to specific points on the phonon dispersion branches of the infinite chain (polymer), treated as a one-dimensional crystal. An analysis has been recently carried out[50] in which specific CC stretching marker bands revealing the distortion from linearity in longer SP[*N*] chains have also been reported.

While the overall IR absorption intensity distribution is comparable for cumulenes and polyynes, Raman spectra

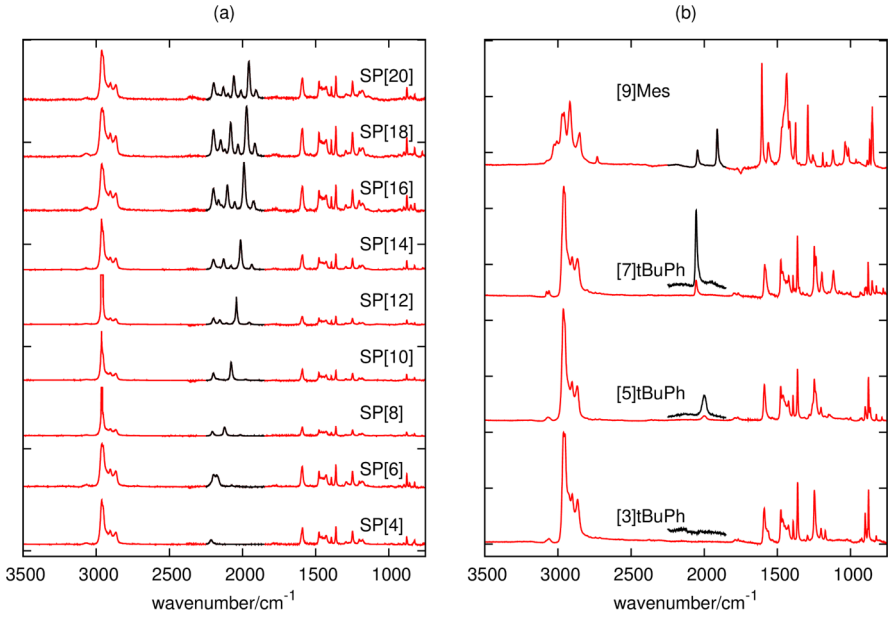

Figure 3. (a) Infrared spectra of SP[N] polyynes series (N = 4–20). (b) Infrared spectra of [n]tBuPh cumulene series (n = 3,5,7) and [9]Mes. Samples are in solid state. For [n]tBuPh, five times magnified spectra in the region of the stretching modes of the linear chains (≈2000 cm^{-1}) are shown. Bands assigned to CC stretching of the linear chain are plotted with a black line.

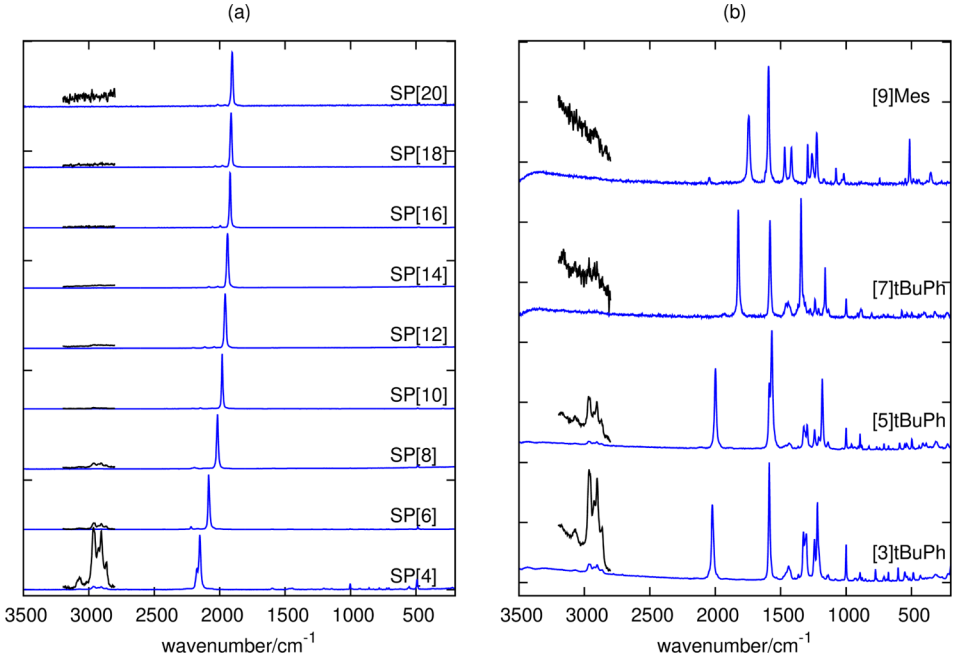

Figure 4. (a) Raman spectra of the SP[N] series (N = 4–20). (b) Raman spectra of the [n]tBuPh cumulene series (n = 3,5,7) and [9]Mes. Samples are in solid state. Magnified spectra in the region of the CH stretching modes are shown (magnification factor of 10 for the [n]tBuPh series and of 20 for SP[N]).

(Figure 4) show remarkable differences between the two classes of molecules. The Raman spectra of SP[N] are very selective, since they are largely dominated by the transition assigned to the so-called "$\mathcal{R}$ mode" (i.e., the BLA oscillation), described by a collective simultaneous out-of-phase CC stretching of the adjacent CC bonds along the sp-carbon chain.[51,55] While for SP[4,6,8] the $\mathcal{R}$ line lies above 2000 cm^{-1}, the CC stretching features of the shorter cumulenes appear in the vicinity of 2000 cm^{-1} and significantly red shift below 2000 cm^{-1} in the longer cumulenes, [7]tBuPh, [9]Mes. Furthermore, cumulenes are characterized by more complicated Raman spectra than polyynes and display several lines of comparable intensity in the region characteristic of the stretchings of conjugated CC bonds (2000–1000 cm^{-1}, see Figure 4). However, for [n]tBuPh series a $\mathcal{R}$ line can be easily recognized simply based on its peak frequency [As shown in ref 27, CC stretching modes of a cumulene chain of finite size can be put in correspondence with properly selected phonons belonging to the acoustical longitudinal dispersion branch of the corresponding ideal polymer, described as a linear monatomic one-dimensional crystal. For cumulene chains containing a relatively small number of C atoms, it results that the $\mathcal{R}$ mode is close to

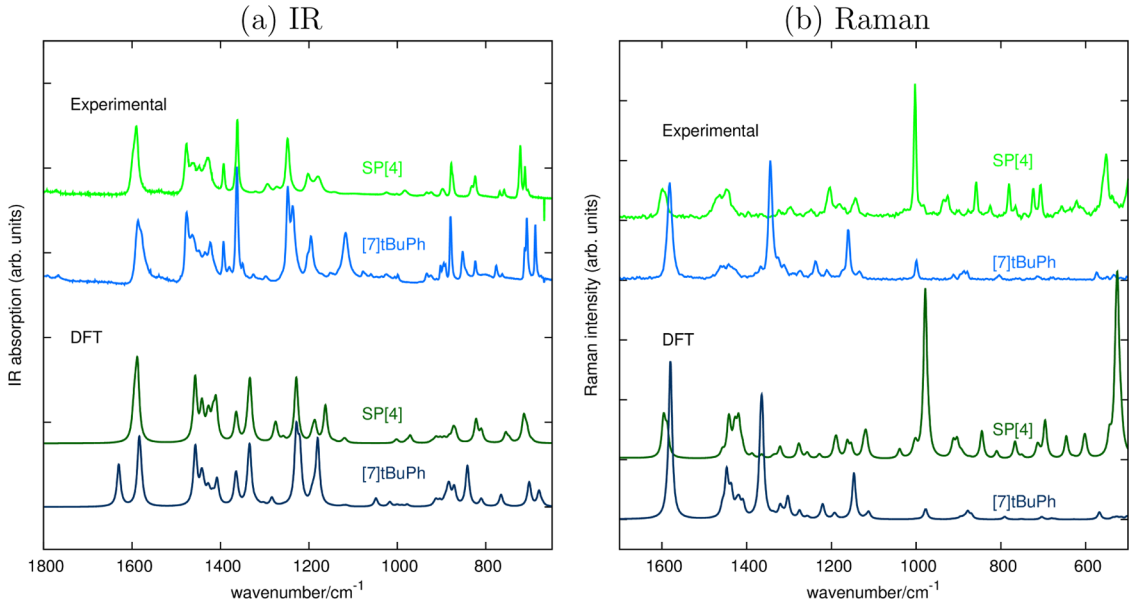

Figure 5. Experimental solid-state and theoretical (DFT, PBE0/6-311G**) vibrational spectra of SP[4] (green lines) and [7]tBuPh (blue lines). (a) Comparison between the experimental IR spectra (top) and their DFT counterparts (bottom) in the 650−1800 cm^{-1} region. (b) Comparison between the experimental Raman spectra (top) and their DFT counterparts (bottom) in the 500−1700 cm^{-1} region. Theoretical IR spectra of SP[4] and [7]tBuPh are plotted adopting the same scale (i.e., intensities of the two molecules can be compared). The theoretical Raman spectrum of SP[4] (dark green line) is magnified by a factor of 25 relative to tBuPh[7] (light green line).

the maximum of the acoustic branch[27] and this is expected to give rise to a higher frequency CC stretching line in the Raman spectrum.]: looking to Figure 4b, we observe that it lies in the range 2000−1800 cm^{-1}. This further supports that cumulene chains behave as more "metallic" systems, which is expected on the basis of the Kohn anomaly predicted for a perfectly equalized infinite chain.[53] Further inspection of Figure 4 reveals that, compared with signals originating from end groups, the strength of the Raman transition associated with the BLA oscillation is very high in polyynes, even in the case of the shorter species available, SP[4]. This feature can be nicely interpreted in the frame of the effective conjugation coordinate (ECC) theory,[55,59] which predicts a very large polarizability change $(\frac{d\alpha}{d\mathcal{R}})$ associated with the BLA oscillation of a π-conjugated chain characterized by a bond alternation pattern. The experimental spectra of cumulenes (Figure 4) show comparatively stronger Raman features in the ring stretching region than polyynes, a feature which could be interpreted as the consequence either of weakening of the Raman activity associated with the $\mathcal{R}$ mode of [n]tBuPh or of a remarkable intensification of the CC stretching features of aryl rings linked to cumulene chains. A closer look to the vibrational features assigned to aryl rings, as reported in Figure 5, can bring to light further interesting experimental evidence. While the infrared spectra of SP[4] and [7]tBu (Figure 5a) show a very similar pattern showing absorption features which roughly maintain the same intensity distribution, the Raman peaks in the same region (Figure 5b) are drastically modified while passing from SP[4] to[7]tBuPh. Few Raman lines of the two molecules can be put in correspondence simply based on frequency position and band shape, as for the IR spectra. However, strong features appear in the Raman spectrum of [7]tBuPh which do not find a counterpart in the Raman spectrum of SP[4]. In particular, two new and strong lines at 1343 and 1160 cm^{-1} are observed in the [7]tBuPh spectrum. In addition, the Raman line of [7]tBuPh at 1582 cm^{-1} shows a non-negligible frequency down shift accompanied by a relative intensity increase. The behavior of the vibrational spectra of [7]tBuPh is similar for all the cumulenes under discussion and the same observations could be extended to the other members of the [n]tBuPh series.

Based on experimental findings, we can state that

(i) CC stretching modes of the [n]tBuPh cumulene chains give rise to Raman transitions of comparable strength with respect to the features found in the ring stretching region and below (Figure 4);

(ii) sizable changes are found over the aryl ring transitions range (1600−1000 cm^{-1}) by comparing the Raman spectra of [n]tBuPh and SP[N] polyynes.

The second point suggests the onset of non-negligible interactions between the cumulene chain and the aryl rings, possibly stronger than those present in polyynes. This concept can be worked out further by considering another piece of experimental evidence, namely the Raman intensity ratio between the ring features and the CH stretching transitions of tBu groups. In spite of the weak Raman intensity measured in the 2800−3000 cm^{-1} region (the spectra become progressively noisier in this region as the chain length increases), it is clear that in [n]tBuPh cumulenes the intensity ratio between the integrated CH stretching Raman band and the ring stretching modes at about 1600 cm^{-1} steadily decreases with chain length n (see Figure 4). Since aliphatic CH stretching intensities of tBu groups can be safely taken as transferrable along the whole [n]tBuPh series, the above observation suggests that the Raman polarizability of the aryl rings is affected by the conjugation length of the cumulated double bonds structure. The last observation can be taken as the experimental evidence that the conjugation path of π electrons of the sp-carbon chain extends somewhat to aryl rings.

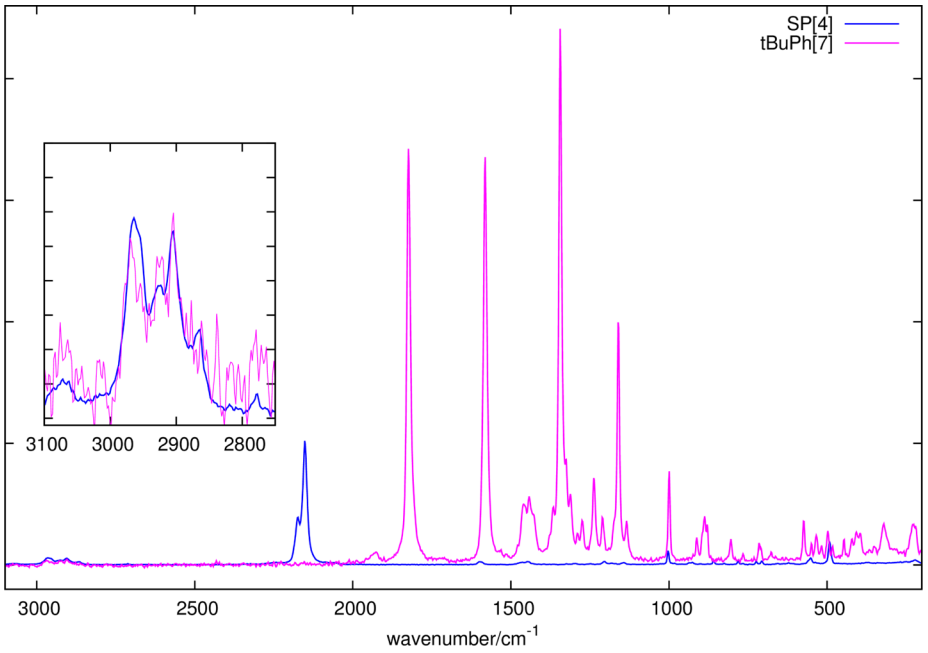

Figure 6. Experimental FT-Raman spectra of polyyne SP[4] and cumulene [7]tBuPh in the solid state, normalized with respect to the aliphatic CH-stretching region (see inset). To increase the signal-to-noise ratio, the spectrum of [7]tBuPh is the average of the six spectra taken at earliest times within the first 30 min right after solvent evaporation (see the Experimental Section of the main text).

In spite of some uncertainty related to the noisy signal over the CH stretching region, it is possible to make a direct comparison between the spectral behavior of SP[4] and [7]tBuPh (e.g., featuring the same number of conjugated bonds) adopting an intensity normalization with respect to the CH stretching signals, as reported in Figure 6. The intensity of aryl modes (ring stretching at 1582 cm^{-1} and breathing at 999 cm^{-1}) in cumulene chains is higher than the polyyne. Moreover, Figure 6 suggests that the intensity of the $\mathcal{R}$ mode is enhanced in the case of the cumulene (compare the Raman line at 2151 cm^{-1} of SP[4] and the line at 1824 cm^{-1} of [7]tBuPh).[63] The above observations support the hypothesis that in cumulenes, such as for the specific case analyzed, [7]tBuPh, the conjugation of the sp-chain extends to aryl groups affecting the molecular polarizability and thus the Raman response. Moreover, we can conclude that the presence of many peaks in the Raman spectrum of cumulenes (different from polyynes) is not ascribed to a weakening of the $\mathcal{R}$ mode intensity, which is comparable to that of a polyyne featuring the same chain length, but it originates by an anomalous intensification of end groups modes.

The experimental intensity data are also presented as a logarithmic plot in Figure 7, which allows visualization of the different trends. Ring stretching and ring breathing modes of the SP[N] species show very small deviations from a constant value, as usually shown by end-modes.[60] A completely different behavior is observed for the analogous normal modes of cumulenes, which show a dramatic increase of their intensity while increasing the chain length. Notice that the ring stretching band of cumulenes follows roughly the same intensity trend of the $\mathcal{R}$ mode, which in turn parallels the intensity behavior of the $\mathcal{R}$ mode of polyynes. Accordingly, we conclude that for [n]tBuPh the three Raman bands here considered are all very sensitive to conjugation and experience a remarkable intensity increase with chain length, while for polyynes SP[N] only the $\mathcal{R}$ line shows this. Quantitative data

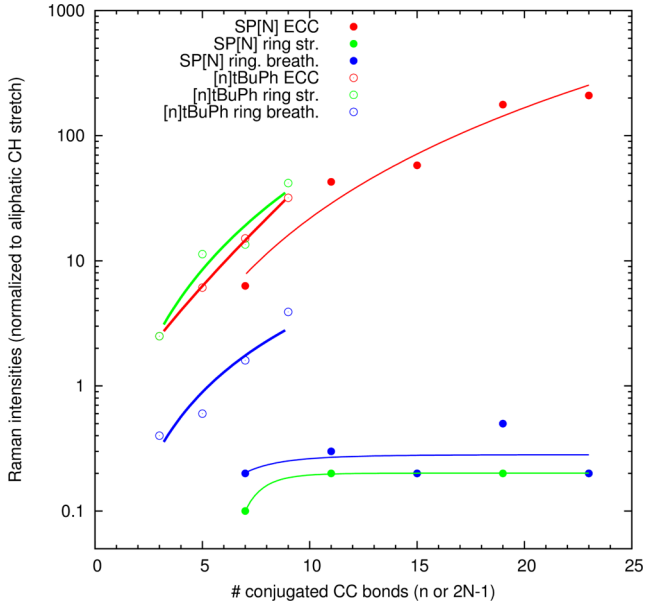

Figure 7. Logarithmic plot of experimental relative Raman intensities in SP[N] polyynes and [n]tBuPh cumulenes (data are presented in Table SI.1). The $\mathcal{R}$ line and two selected Raman lines in the aryl stretching region are considered, namely the ring stretching line at about 1600 cm^{-1} and the ring breathing at about 1000 cm^{-1}. See text for discussion.

obtained by the analysis of the integrated Raman intensities (normalized to CH stretching intensities) for the entire series of SP[N] and [n]tBuPh are reported in the Supporting Information (Table SI.1).

The interplay between the two π electrons systems, rings and carbon chain, is further supported by the comparison between the frontier orbitals of [7]tBuPh and SP[4], as reported in Figure 8. Indeed the wave functions extend more over the aryl groups while passing from SP[4] to tBuPh[7] and [9]Mes.

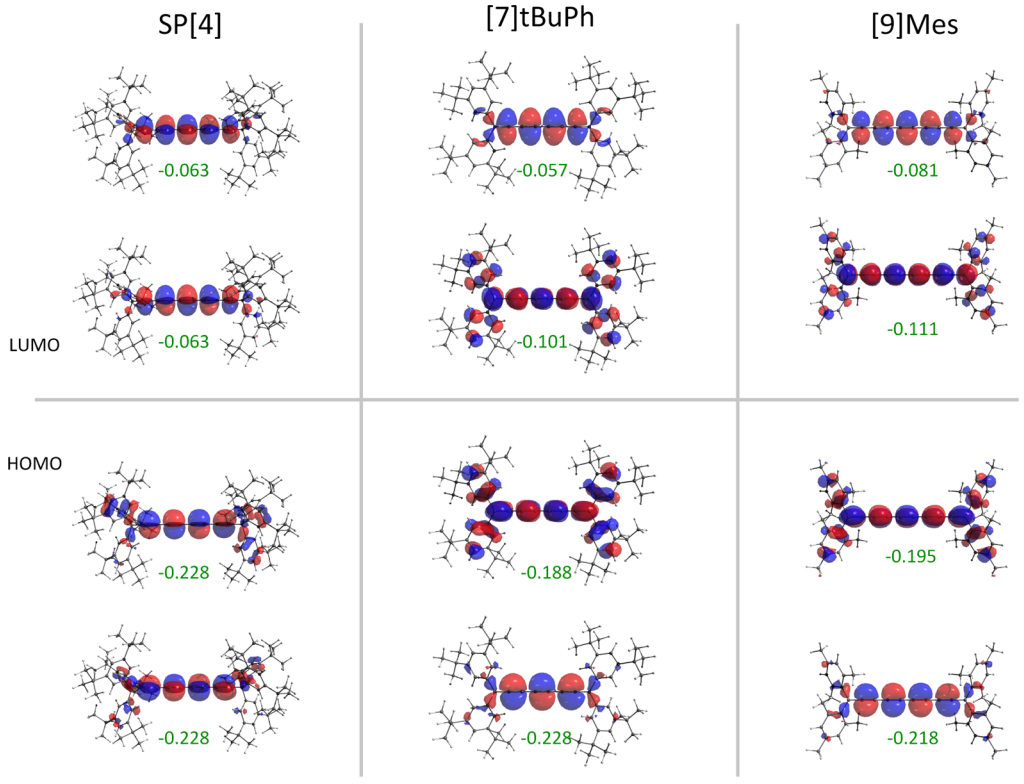

Figure 8. Frontier orbitals of SP[4] polyyne (left column), [7]tBuPh (central column), and [9]Mes cumulene (right column), from PBE0/6-311G** DFT calculations. The energies of the orbitals are reported in atomic units.

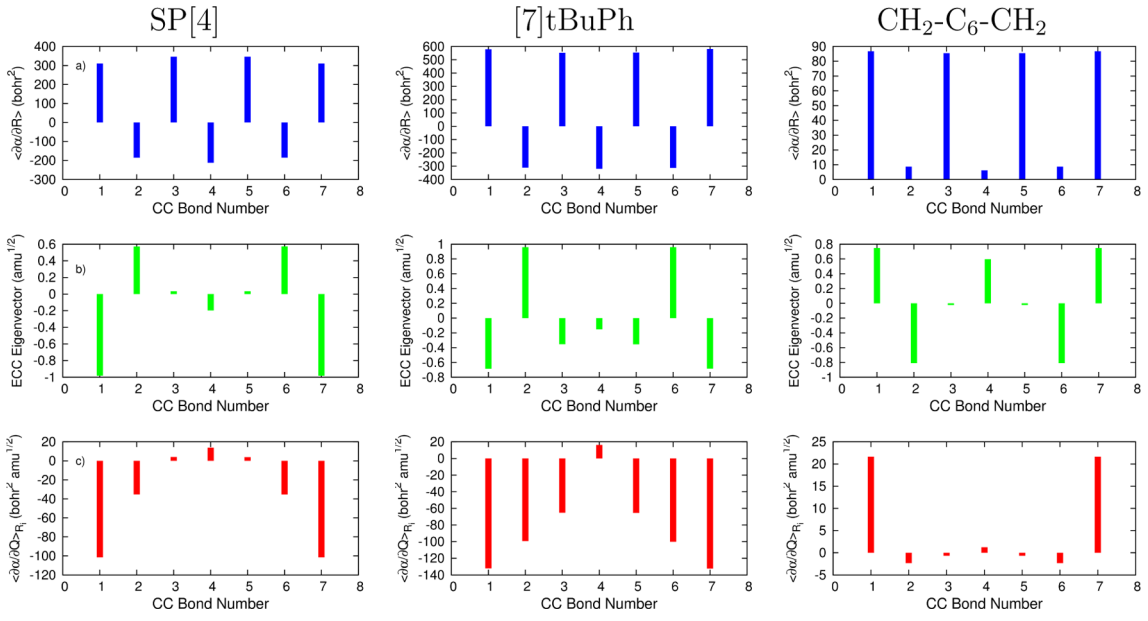

Figure 9. Comparison of computed Raman parameters relative to the CC bonds along the cumulene chain for three molecules characterized by a conjugated linear chain of the same length: SP[4], [7]tBuPh, and $CH_2-C_6-CH_2$. Results from DFT calculations (PBE0/6-311G**). From top to bottom: (a) trace of the CC stretching polarizability tensor $\mathrm{Tr}(d\alpha/d\mathcal{R})$; (b) weight of the individual contribution of CC stretching to the $\mathcal{R}$ mode eigenvector; (c) individual contribution of CC stretching to the total polarizability of the $\mathcal{R}$ mode. CC bonds are numbered following the conjugated chain path from one end to the other one, consistent with Figure 2b.

Furthermore, the local symmetry of the sp chain (supposed linear) loses the C_3 axis as in SP[4], becoming a C_2 axis in [7]tBuPh and [9]Mes. On this basis, we observe the removal of HOMO/HOMO−1 (LUMO/LUMO−1) degeneracy while passing from trityl capped polyynes to aryl end-capped cumulenes. Indeed, out of the two π-systems of the sp-chain, only one (π_x) can effectively couple to the aryl groups, since $2p_x$ orbitals of the sp-carbons are oriented closer to the $2p$ orbitals of the aryl carbons (see Figure 8), giving rise to the highly delocalized HOMO and LUMO orbitals of [n]tBuPh. The interaction with aryl units not only removes the degeneracy between the frontier molecular orbitals but also dramatically

lowers the HOMO−LUMO gap of aryl end-capped cumulene ($gap_{SP[4]}$ = 0.16 ha, $gap_{[7]tBuPh}$ = 0.09 ha). The extension of the electron conjugation to the aryl groups has profound consequences also on the Raman response and on the vibrational dynamics of the molecule, resulting in couplings between vibrational displacements of the cumulene chain and of the aryl rings. These effects will be discussed in detail in the next section, looking at vibrational displacements provided by DFT calculations.

BOND POLARIZABILITY DERIVATIVES AND MOLECULAR STRUCTURE

Despite of the fact that polarizability derivatives along CC stretchings of the chain are overestimated by DFT in both [*n*]tBuPh and SP[*N*] polyynes (see Supporting Information for details), interesting information on π-conjugation and end group effects can be gained by looking at the computed Raman bond parameters, namely $d\alpha/dR_j$ (where R_j is one of the CC stretching coordinates along the sp-chain). These are responsible for the large Raman cross section of totally symmetric CC stretching normal modes. We address here the rationalization for the fact that experimental intensity data and, to a larger extent, theoretical predictions tell us that [*n*]tBuPh cumulenes show strong $\mathcal{R}$ modes, comparable to those observed for polyynes, in contrast to simpler model cumulenes discussed in ref 27. [In ref 27 the following were predicted: (1) a noticeable weakening of the Raman activity of the $\mathcal{R}$ mode of vinylidene end-capped cumulenes, always accompanied by a loss of selectivity of the calculated Raman spectra and (2) a rationalization of such behavior in terms of local Raman parameters. However, that was a theoretical investigation on model cumulenic systems. Here we can, for the first time, experimentally assess theoretical predictions on synthesized cumulene molecules featuring known chain length and structure.] In Figure 9 we report a synopsis of the main invariant of the polarizability derivatives, $\mathrm{Tr}(d\alpha/dR_j)$, that determines the Raman activities of the CC stretching modes. For details about this procedure in other systems see refs 55 and 57. We compare three different sp-chains with comparable lengths: two cumulenes ([7]tBuPh and its vinylidene end-capped counterpart) and SP[4] polyyne. The inspection of the three top panels of Figure 9a reveals similar trends for SP[4] and [7]tBuPh: both molecules show a well-known alternating behavior, which is usually found in π-conjugated carbon chains characterized by a sequence of short and long bonds. In these systems it is typical to observe an oscillating pattern of positive and negative values of $d\alpha_{zz}/dR_j$ along the chain axis *z*. Usually the *zz* component is dominant, so that $\mathrm{Tr}(d\alpha/dR_j) \approx d\alpha_{zz}/dR_j$.[27,55] We also observe in Figure 9a that [7]tBuPh and SP[4] show comparable values, while the vinylidene end-capped cumulene is characterized by markedly lower polarizability derivatives (by about a factor of 10).

By considering the individual CC stretching contributions ($L_{j\mathcal{R}}$) in the nuclear displacements of the $\mathcal{R}$ modes, it is possible to explain the large polarizability change associated with the $\mathcal{R}$ mode of SP[4] and [7]tBuPh. In fact, each $d\boldsymbol{\alpha}/dR_j$ value constructively adds up to determine the total polarizability change, since $d\boldsymbol{\alpha}/d\mathcal{R} = \sum_j d\boldsymbol{\alpha}/dR_j L_{j\mathcal{R}}$.[55] This is clearly illustrated in the panels of Figure 9b and c, which show the pattern of $L_{j\mathcal{R}}$ coefficients and the products $d\boldsymbol{\alpha}/d\mathcal{R}_j \cdot L_{j\mathcal{R}}$ for the strong $\mathcal{R}$ modes computed in SP[4] and [7]tBuPh. The values of the polarizability derivatives reported in Figure 9 also justify the trend of the Raman activities of the $\mathcal{R}$ bands in SP[4] ($I_{\mathcal{R}}$ = 146311 A^4 amu^{-1}) and [7]tBuPh: ($I_{\mathcal{R}}$ = 322198 A^4 amu^{-1}).

The pattern of $\mathrm{Tr}(d\alpha/dR_j)$ values in the vinylidene end-capped cumulene is remarkably different (Figure 9a), with values lower by about 1 order of magnitude and positive signs all along the sp-chain. This pattern is consistent with previous theoretical work[27] and with the "metallic" character of the chain, showing very low BLA value at the equilibrium geometry: in other words, a chain consisting of quasi equivalent CC bonds should exhibit bond parameters (e.g., $\mathrm{Tr}(d\alpha/dR_j)$) close in value, or at least with the same sign.[27] This feature is even more remarkable if one considers that, in the limit of a perfectly equalized infinite monatomic chain, the $\mathcal{R}$ mode is Raman silent for symmetry reasons, since it corresponds to the $q = \pi/a \neq 0$ longitudinal phonon. The fact that [7]tBuPh and $CH_2-C_6-CH_2$ show significantly different Raman parameters (Figure 9), even if they possess similar and low BLA, suggests that the transition between the alternated bond length regime and a truly metallic regime occurs in a very narrow range of BLA values, close to zero.

The observed trends of local Raman parameters can be analyzed further by considering the role of the frontier orbitals in determining the values of the polarizability derivatives. This is done by considering the pattern of the bond-order changes upon excitation.[61] Nodal analysis of the frontier orbitals reveals the bonding/antibonding contributions along the sp-chain and how they are modified upon low-lying transitions. We conclude that, compared to vinylidene end-capped cumulene $CH_2-C_6-CH_2$, the loss of the HOMO degeneracy caused by the coupling with π-electrons of the aryl groups is the fundamental reason for the different Raman behavior of [*n*]tBuPh (see Supporting Information). On this ground we can state that in aryl cumulenes the sign pattern of the $\mathrm{Tr}(d\alpha/dR_j)$ parameters can be deduced by considering how the nodal planes are modified while passing from HOMO to LUMO (see Figure 8 and Supporting Information). The high values of the polarizability parameters and of the Raman intensity of the $\mathcal{R}$ mode are justified by the fact that the π-orbitals of the aryl groups concur to determine (i) an effective energy separation between the HOMO and HOMO−1 levels and (ii) an important enhancement of the molecular polarizability (and of its derivatives) thanks to the increase of the conjugation length extending outside the sp-carbon chain. The relevant contribution of the aryl groups to the highly delocalized frontier orbitals of [7]tBuPh also justifies the strong increase of the Raman activity associated with the CC stretching modes of the aryl groups, compared to what happens in polyyne SP[4] (which displays weaker aryl ring stretching modes). As a consequence of the above analysis, we argue that a modulation of the end group conformation while changing the values of the dihedral angles which control the orientation of the aryl units may be used as a strategy to modulate the π-conjugation and spectroscopic response of the sp-carbon chain. Similarly, a substitution with electron donor/acceptor groups on the aryl end-capping groups could be used to polarize the sp-chain through the π-conjugation effects, as described above.

CONCLUSIONS

Based on the experimental data collected for [*n*]tBuPh and SP[*N*] series and the associated results from DFT calculations, we can state the following points:

(i) The experimental Raman spectra of [n]tBuPh are characterized by a remarkably low wavenumber of the $\mathcal{R}$ band and can be taken as the spectroscopic signature of the transition of cumulenes toward a "metallic" regime. This is consistent with the measured optical gaps, which are significantly lower than those of polyynes.[24]

(ii) In spite of their equalized CC bonds, [n]tBuPh cumulenes display a strong Raman intensity of the $\mathcal{R}$ mode. The analysis of the computed bond polarizability derivatives ($d\alpha/dR_j$) provides a reasonable rationalization of this fact. The pattern of the $d\alpha/dR_j$ parameters along the sp-carbon chain unexpectedly indicates that [n]tBuPh, from the point of view of the Raman response, obey a regime typical of the systems characterized by alternated CC bonds. This behavior is caused by the fact that the frontier orbitals extend to the aryl moieties of the end groups.

(iii) Experiments and calculations reveal a remarkable increase of the Raman intensity of the modes of the aryl rings in [n]tBuPh cumulenes compared to polyynes with the same end-capping groups. This is a further proof that in [n]tBuPh cumulenes, π-conjugation of the sp-carbon sequence also extends to the aryl rings of the end groups. The contribution from the linear chain to the Raman activity in the characteristic region of the aryl-ring modes is 2-fold: (1) CC stretching of the chains is involved in aryl modes through an effective vibrational coupling; (2) π electrons of the sp-chain contribute to the increase of the molecular polarizability and its derivatives with respect to CC stretching coordinates of the aryl ring.

Within the picture proposed here we finally note a relevant issue that applies to the detection and study of cumulenic structures embedded in nanostructured sp/sp^2 carbon materials (i.e., also containing graphitic domains). Based on our conclusions we can state that their spectroscopic response is strongly influenced by the nature of the carbon structures bonded at the ends of the sp-carbon chains.[26−28] If a conjugation path that extends to the π-system of condensed aromatic rings becomes available through chain ends, we expect a remarkable activation of otherwise silent (or very weak) Raman transitions. This phenomenon can also occur in the case of relatively long chains, for which no allowed Raman transitions are predicted if they are modeled as ideally infinite, monatomic chain crystals.

ASSOCIATED CONTENT

Supporting Information

Details on DFT calculations of the vibrational spectra, Raman intensities, and polarizability derivatives. This material is available free of charge via Internet.

AUTHOR INFORMATION

Corresponding Author

*E-mail: matteo.tommasini@polimi.it.

Notes

The authors declare no competing financial interest.

ACKNOWLEDGMENTS

The authors are grateful for funding from the Deutsche Forschungsgemeinschaft (DFG SFB 953, Synthetic Carbon Allotropes), the Interdisciplinary Center for Molecular Materials (ICMM), and the Excellence Initiative, supporting the Cluster of Excellence Engineering of Advanced Materials. D.F. acknowledges the Alexander von Humboldt foundation for a post-doctoral fellowship.

REFERENCES

(1) Shi Shun, A. L. K.; Tykwinski, R. R. Synthesis of Naturally Occurring Polyynes. *Angew. Chem., Int. Ed.* **2006**, *45*, 1034−1057.

(2) Pan, Y.; Lowary, T. L.; Tykwinski, R. R. Naturally Occurring and Synthetic Polyyne Glycosides. *Can. J. Chem.* **2009**, *87*, 1565−1582.

(3) Gung, B. W. Total Synthesis of Polyyne Natural Products. *C. R. Chim.* **2009**, *12*, 489−505.

(4) Whittaker, A. G.; Watts, E. J.; Lewis, R. S.; Anders, E. Carbynes: Carriers of Primordial Noble Gases in Meteorites. *Science* **1980**, *209*, 1512−1514.

(5) Hayatsu, R.; Scott, R. G.; Studier, M. H.; Lewis, R. S.; Anders, E. Carbynes in Meteorites: Detection, Low-Temperature Origin, and Implications for Interstellar Molecules. *Science* **1980**, *209*, 1515−1518.

(6) Webster, A. Carbyne as a Possible Constituent of the Interstellar Dust. *Mon. Not. R. Astron. Soc.* **1980**, *192*, 7−9.

(7) Ravagnan, L.; Siviero, F.; Lenardi, C.; Piseri, P.; Barborini, E.; Milani, P.; Casari, C. S.; Li Bassi, A.; Bottani, C. E. Cluster-Beam Deposition and in situ Characterization of Carbyne-Rich Carbon Films. *Phys. Rev. Lett.* **2002**, *89*, 285506.

(8) Ravagnan, L.; Piseri, P.; Bruzzi, M.; Miglio, S.; Bongiorno, G.; Baserga, A.; Casari, C. S.; Li Bassi, A.; Lenardi, C.; Yamaguchi, Y.; et al. Influence of Cumulenic Chains on the Vibrational and Electronic Properties of *sp*−*sp*^{2} Amorphous Carbon. *Phys. Rev. Lett.* **2007**, *98*, 216103.

(9) Casari, C. S.; Li Bassi, A.; Baserga, A.; Ravagnan, L.; Piseri, P.; Lenardi, C.; Tommasini, M.; Milani, A.; Fazzi, D.; Bottani, C. E.; et al. Low-Frequency Modes in the Raman Spectrum of *sp*−*sp*^{2} Nanostructured Carbon. *Phys. Rev. B* **2008**, *77*, 195444.

(10)Zhao, X.; Ando, Y.; Liu, Y.; Jinno, M.; Suzuki, T. Carbon Nanowire Made of a Long Linear Carbon Chain Inserted Inside a Multiwalled Carbon Nanotube. *Phys. Rev. Lett.* **2003**, *90*, 187401.

(11)Scuderi, V.; Scalese, S.; Bagiante, S.; Compagnini, G.; D'Urso, L.; Privitera, V. Direct Observation of the Formation of Linear C Chain/Carbon Nanotube Hybrid Systems. *Carbon* **2009**, *47*, 2134− 2137.

(12)Jin, C.; Lan, H.; Peng, L.; Suenaga, K.; Iijima, S. Deriving Carbon Atomic Chains from Graphene. *Phys. Rev. Lett.* **2009**, *102*, 205501.

(13)Lagow, R. J.; Kampa, J. J.; Wei, H.-C.; Battle, S. L.; Genge, J. W.; Laude, D. A.; Harper, C. J.; Bau, R.; Stevens, R. C.; Haw, J. F.; et al. Synthesis of Linear Acetylenic Carbon: The "sp" Carbon Allotrope. *Science* **1995**, *267*, 362−367.

(14)Cataldo, F. Polyynes and Cyanopolyynes Synthesis from the Submerged Electric Arc: about the Role Played by the Electrodes and Solvents in Polyynes Formation. *Tetrahedron* **2004**, *60*, 4265−4274.

(15)Cataldo, F., Ed. *Polyynes: Synthesis, Properties and Applications*; CRC Taylor & Francis: Boca Raton, FL, 2006.

(16)Cataldo, F.; Casari, C. S. Synthesis, Structure and Thermal Properties of Copper and Silver Polyynides and Acetylides. *J. Inorg. Organomet. Polym. Mater.* **2007**, *17*, 641−651.

(17)Chalifoux, W. A.; Tykwinski, R. R. Synthesis of Polyynes To Model the sp-Carbon Allotrope Carbyne. *Nat. Chem.* **2010**, *2*, 967−971.

(18)Sato, Y.; Kodama, T.; Shiromaru, H.; Sanderson, J.; Fujino, T.; Wada, Y.; Wakabayashi, T.; Achiba, Y. Synthesis of Polyyne Molecules from Hexane by Irradiation of Intense Femtosecond Laser Pulses. *Carbon* **2010**, *48*, 1673−1676.

(19)Wesolowski, M.; Kuzmin, S.; Moores, B.; Wales, B.; Karimi, R.; Zaidi, A.; Leonenko, Z.; Sanderson, J.; Duley, W. Polyyne Synthesis and Amorphous Carbon Nano-Particle Formation by Femtosecond Irradiation of Benzene. *Carbon* **2011**, *49*, 625−630.

(20)Hu, A.; Rybachuk, M.; Lu, Q.-B.; Duley, W. W. Direct Synthesis of sp-Bonded Carbon Chains on Graphite Surface by Femtosecond Laser Irradiation. *Appl. Phys. Lett.* **2007**, *91*, 131906.

(21) Heimann, R. B., Evsyukov, S. E., Kavan, L., Eds. *Carbyne and Carbynoid Structures*; Kluwer Academic Publishers: Dordrecht, The Netherlands, 1999.
(22) Szafert, S.; Gladysz, J. A. Carbon in One Dimension: Structural Analysis of the Higher Conjugated Polyynes. *Chem. Rev.* **2003**, *103*, 4175−4206, PMID: 14611262.
(23) Chalifoux, W. A.; Tykwinski, R. R. Synthesis of Extended Polyynes: Toward Carbyne. *C. R. Chim.* **2009**, *12*, 341−358.
(24) Januszewski, J. A.; Wendinger, D.; Methfessel, C. D.; Hampel, F.; Tykwinski, R. R. Synthesis and Structure of Tetraarylcumulenes: Characterization of Bond-Length Alternation versus Molecule Length. *Angew. Chem., Int. Ed.* **2013**, *52*, 1817−1821.
(25) Januszewski, J. A.; Tykwinski, R. R. Synthesis and Properties of Long [n]Cumulenes ($n \geq 5$). *Chem. Soc. Rev.* **2014**, *43*, 3184−3203.
(26) Ravagnan, L.; Manini, N.; Cinquanta, E.; Onida, G.; Sangalli, D.; Motta, C.; Devetta, M.; Bordoni, A.; Piseri, P.; Milani, P. Effect of Axial Torsion on sp-Carbon Atomic Wires. *Phys. Rev. Lett.* **2009**, *102*, 245502.
(27) Innocenti, F.; Milani, A.; Castiglioni, C. Can Raman Spectroscopy Detect Cumulenic Structures of Linear Carbon Chains? *J. Raman Spectrosc.* **2010**, *41*, 226−236.
(28) Milani, A.; Lucotti, A.; Russo, V.; Tommasini, M.; Cataldo, F.; Li Bassi, A.; Casari, C. S. Charge Transfer and Vibrational Structure of sp-Hybridized Carbon Atomic Wires Probed by Surface Enhanced Raman Spectroscopy. *J. Phys. Chem. C* **2011**, *115*, 12836−12843.
(29) Yildizhan, M. M.; Fazzi, D.; Milani, A.; Brambilla, L.; Del Zoppo, M.; Chalifoux, W. A.; Tykwinski, R. R.; Zerbi, G. Photogenerated Cumulenic Structure of Adamantyl Endcapped Linear Carbon Chains: An Experimental and Computational Investigation Based on Infrared Spectroscopy. *J. Chem. Phys.* **2011**, *134*, 124512.
(30) Lang, N. D.; Avouris, P. Carbon-Atom Wires: Charge-Transfer Doping, Voltage Drop, and the Effect of Distortions. *Phys. Rev. Lett.* **2000**, *84*, 358−361.
(31) Crljen, Z.; Baranovic, G. Unusual Conductance of Polyyne-Based Molecular Wires. *Phys. Rev. Lett.* **2007**, *98*, 116801.
(32) Liu, M.; Artyukhov, V. I.; Lee, H.; Xu, F.; Yakobson, B. I. Carbyne from First Principles: Chain of C Atoms, a Nanorod or a Nanorope. *ACS Nano* **2013**, *7*, 10075−10082.
(33) Ermer, S. P.; Lovejoy, S. M.; Leung, D. S.; Altman, J. C.; Aron, K. P.; Spitzer, R. C.; Hansen, G. A. Synthesis and Evaluation of Cumulenes: Novel Rigid Nonlinear Optical Molecules. *Proc. SPIE* **1990**, *1337*, 89−98.
(34) Kminek, I.; Klimovic, J.; Prasad, P. N. Third-Order Nonlinear Optical Response of Some Tetrasubstituted Cumulenes. *Chem. Mater.* **1993**, *5*, 357−360.
(35) Eisler, S.; Slepkov, A. D.; Elliott, E.; Luu, T.; McDonald, R.; Hegmann, F. A.; Tykwinski, R. R. Polyynes as a Model for Carbyne: Synthesis, Physical Properties, and Nonlinear Optical Response. *J. Am. Chem. Soc.* **2005**, *127*, 2666−2676, PMID: 15725024.
(36) Lucotti, A.; Tommasini, M.; Fazzi, D.; Del Zoppo, M.; Chalifoux, W. A.; Tykwinski, R. R.; Zerbi, G. Absolute Raman Intensity Measurements and Determination of the Vibrational Second Hyperpolarizability of Adamantyl Endcapped Polyynes. *J. Raman Spectrosc.* **2012**, *43*, 1293−1298.
(37) Lang, N. D.; Avouris, P. Oscillatory Conductance of Carbon-Atom Wires. *Phys. Rev. Lett.* **1998**, *81*, 3515−3518.
(38) Ballmann, S.; Hieringer, W.; Secker, D.; Zheng, Q.; Gladysz, J. A.; Görling, A.; Weber, H. B. Molecular Wires in Single-Molecule Junctions: Charge Transport and Vibrational Excitations. *ChemPhysChem* **2010**, *11*, 2256−2260.
(39) Börrnert, F.; Börrnert, C.; Gorantla, S.; Liu, X.; Bachmatiuk, A.; Joswig, J.-O.; Wagner, F. R.; Schäffel, F.; Warner, J. H.; Schönfelder, R.; et al. Single-Wall-Carbon-Nanotube/Single-Carbon-Chain Molecular Junctions. *Phys. Rev. B* **2010**, *81*, 085439.
(40) Nair, A. K.; Cranford, S. W.; Buehler, M. J. The Minimal Nanowire: Mechanical Properties of Carbyne. *Europhys. Lett.* **2011**, *95*, 16002.
(41) Akdim, B.; Pachter, R. Switching Behavior of Carbon Chains Bridging Graphene Nanoribbons: Effects of Uniaxial Strain. *ACS Nano* **2011**, *5*, 1769−1774.
(42) Ataca, C.; Ciraci, S. Perpendicular Growth of Carbon Chains on Graphene from First-Principles. *Phys. Rev. B* **2011**, *83*, 235417.
(43) Moreno-Garca, P.; Gulcur, M.; Manrique, D. Z.; Pope, T.; Hong, W.; Kaliginedi, V.; Huang, C.; Batsanov, A. S.; Bryce, M. R.; Lambert, C.; et al. Single-Molecule Conductance of Functionalized Oligoynes: Length Dependence and Junction Evolution. *J. Am. Chem. Soc.* **2013**, *135*, 12228−12240.
(44) Cretu, O.; Botello-Mendez, A. R.; Janowska, I.; Pham-Huu, C.; Charlier, J.-C.; Banhart, F. Electrical Transport Measured in Atomic Carbon Chains. *Nano Lett.* **2013**, *13*, 3487−3493.
(45) Prasongkit, J.; Grigoriev, A.; Ahuja, R. Mechano-Switching Devices from Carbon Wire-Carbon Nanotube Junctions. *Phys. Rev. B* **2013**, *87*, 155434.
(46) Rivelino, R.; dos Santos, R. B.; de Brito Mota, F.; Gueorguiev, G. K. Conformational Effects on Structure, Electron States, and Raman Scattering Properties of Linear Carbon Chains Terminated by Graphene-Like Pieces. *J. Phys. Chem. C* **2010**, *114*, 16367−16372.
(47) Tabata, H.; Fujii, M.; Hayashi, S.; Doi, T.; Wakabayashi, T. Raman and Surface-Enhanced Raman Scattering of a Series of Size-Separated Polyynes. *Carbon* **2006**, *44*, 3168−3176.
(48) Wakabayashi, T.; Murakami, T.; Nagayama, H.; Nishide, D.; Kataura, H.; Achiba, Y.; Tabata, H.; Hayashi, S.; Shinohara, H. Raman Spectral Features of Longer Polyynes $HC_{2n}H$ (n = 4−8) in SWNTs. *Eur. Phys. J. D* **2009**, *52*, 79−82.
(49) Wada, Y.; Morisawa, Y.; Wakabayashi, T. Spectroscopic Characterization of a Series of Polyyne-Iodine Molecular Complexes $H(CC)_nH(I_6)$ of n = 5−9. *Chem. Phys. Lett.* **2012**, *541*, 54−59.
(50) Agarwal, N. R.; Lucotti, A.; Fazzi, D.; Tommasini, M.; Castiglioni, C.; Chalifoux, W.; Tykwinski, R. R. Structure and Chain Polarization of Long Polyynes Investigated with Infrared and Raman Spectroscopy. *J. Raman Spectrosc.* **2013**, *44*, 1398−1410.
(51) Lucotti, A.; Tommasini, M.; Fazzi, D.; Del Zoppo, M.; Chalifoux, W. A.; Ferguson, M. J.; Zerbi, G.; Tykwinski, R. R. Evidence for Solution-State Nonlinearity of sp-Carbon Chains Based on IR and Raman Spectroscopy: Violation of Mutual Exclusion. *J. Am. Chem. Soc.* **2009**, *131*, 4239−4244.
(52) Yang, S.; Kertesz, M. Bond Length Alternation and Energy Band Gap of Polyyne. *J. Phys. Chem. A* **2006**, *110*, 9771−9774, PMID: 16884210.
(53) Milani, A.; Tommasini, M.; Del Zoppo, M.; Castiglioni, C.; Zerbi, G. Carbon Nanowires: Phonon and π-Electron Confinement. *Phys. Rev. B* **2006**, *74*, 153418.
(54) Frisch, M. J.; Trucks, G. W.; Schlegel, H. B.; Scuseria, G. E.; Robb, M. A.; Cheeseman, J. R.; Scalmani, G.; Barone, V.; Mennucci, B.; Petersson, G. A. et al. *Gaussian 09*, Revision D.01; Gaussian Inc.: Wallingford, CT, 2009.
(55) Castiglioni, C.; Tommasini, M.; Zerbi, G. Raman Spectroscopy of Polyconjugated Molecules and Materials: Confinement Effect in One and Two Dimensions. *Philos. Trans. R. Soc. A* **2004**, *362*, 2425− 2459.
(56) Radice, S.; Tommasini, M.; Castiglioni, C. Two Dimensional Correlation Raman Spectroscopy of Perfluoropolyethers: Effect of Peroxide Groups. *J. Mol. Struct.* **2010**, *974*, 73−79.
(57) Johannessen, C.; Blanch, E. W.; Villani, C.; Abbate, S.; Longhi, G.; Agarwal, N. R.; Tommasini, M.; Lightner, D. A.; Raman, R. O. A. Spectra of (−)- and (+)-2-Br-Hexahelicene: Experimental and DFT Studies of a π-Conjugated Chiral System. *J. Phys. Chem. B* **2013**, *117*, 2221−2230.
(58) Tykwinski, R. R.; Chalifoux, W.; Eisler, S.; Lucotti, A.; Tommasini, M.; Fazzi, D.; Del Zoppo, M.; Zerbi, G. Toward Carbyne: Synthesis and Stability of Really Long Polyynes. *Pure Appl. Chem.* **2010**, *82*, 891−904.
(59) Castiglioni, C.; Lopez Navarrete, J.; Zerbi, G.; Gussoni, M. A Simple Interpretation of the Vibrational Spectra of Undoped, Doped and Photoexcited Polyacetylene: Amplitude Mode Theory in the GF Formalism. *Solid State Commun.* **1988**, *65*, 625−630.

(60) Castiglioni, C. In *Vibrational Spectroscopy of Polymers: Principles and Practice*; Everall, N., Griffiths, P. R., Chalmers, J. M., Eds.; Wiley: 2007.
(61) Tommasini, M.; Castiglioni, C.; Zerbi, G. Raman Scattering of Molecular Graphenes. *Phys. Chem. Chem. Phys.* **2009**, *11*, 10185–10194.
(62) In the case of [9]Mes the CH stretching band, ascribed to modes localized on methyl groups directly linked to the aryl rings, is comparatively weaker with respect to the [*n*]tBuPh series, because of the reduced number of CH oscillators; moreover, in this case, hyperconjugation to the π-system can affect IR absorption intensities and band shapes.
(63) The normalization to CH stretching intensity is not completely suitable for a comparison of the $\mathcal{R}$ mode intensity in cumulenes and polyynes; indeed, while intensity ratios of bands associated with group modes of aryl units (e.g., CH stretching and ring stretchings) are independent from the number of aryl units in the molecule, the intensities of chain modes (i.e., the $\mathcal{R}$ mode) of SP[4] and [7]tBuPh are "measured" in Figure 6 with reference to the scattering from 108 and 72 CH stretching oscillators (respectively). A scaling of the intensity ratios taking into account the different number of CH oscillators in the two molecules allows evaluating a "corrected" intensity ratio for the $\mathcal{R}$ line of 1.6 (see also Table 1) to be compared with the factor of 2.4, obtained according to the intensity scale adopted in Figure 6.